

SHORT COMMUNICATION

PREPARATION, CHARACTERIZATION AND OPTICAL PROPERTIES OF MCM-41/RHODAMINE B

Yue-Xiang Liu and Qing-Zhou Zhai*

Research Center for Nanotechnology, Changchun University of Science and Technology,
Changchun 130022, P.R. China

(Received May 1, 2008; revised September 17, 2008)

ABSTRACT. Nanometer MCM-41 molecular sieve and rhodamine B (RhB) have been used for the host and guest, respectively, to prepare host-guest (nanometer MCM-41)-RhB composite materials by liquid-phase grafting method. Powder X-ray diffraction, chemical analysis, infrared spectroscopy, low temperature nitrogen adsorption-desorption technique and diffuse reflectance absorption spectroscopy were used to characterize the prepared (nanometer MCM-41)-RhB host-guest composite material. The results showed that the framework of the molecular sieve in the host-guest composite material is well retained and highly ordered. The RhB was confined and dispersed inside the channels of the host material. A blue-shift of 56 nm in the UV-vis diffuse reflection absorption spectrum of the host-guest composite material prepared further indicated that RhB trapped in the channels of the molecular sieve. The guest was stereoscopically confined by the channels of the nanometer MCM-41 host. The prepared host-guest composite material shows luminescence. The material has the potentiality as luminescence material.

KEY WORDS: Host-guest nanocomposite material, Nanometer MCM-41 molecular sieve host, Rhodamine B guest, Characterization, Luminescence

INTRODUCTION

Nanomaterials have some wonderful properties, showing specially optical, electrical and magnetic performance [1-5]. Zeolites are one family of materials with nanodimension pores, which are considered as very good templates for preparing quantum dots and nano quantum wires. The micron mesoporous MCM-41 molecular sieve material was synthesized by Mobil Company in 1992 and this discovery represents molecular sieve mesoporous materials to come into new times [6, 7]. The investigation of MCM-41 caused great interests and in 2001 Cai *et al.* [8] successfully prepared nanoscale MCM-41 molecular sieves. The nanometer molecular sieve has big and adjusted pore diameters, good thermal stability, high specific surface and good adsorptive capacity. The nanometer MCM-41 mesoporous materials are expected to show their great potentiality and diversity in adsorption, separation and catalytic activity. The perfect periodic nanostructures of the mesoporous molecular sieves make themselves become the ideal hosts for nanomanufacturing [9-11]. Rhodamine B (RhB) is extensively used in the areas of optics and laser as a type of organic dye. Served as a kind of good fluorescence compound, RhB shows very good stability and has high efficiency in fluorescent quantum effect. The MCM-41 molecular sieves have been modified [12, 13] and incorporated by some guests such as ferrocenyl dendrimers [14], silver iodide [15]. In this study, the nanometer MCM-41 was used as host and rhodamine B (RhB) as guest to prepare (MCM-41)-RhB host-guest composite material by liquid-phase grafting method. The powder X-ray diffraction, chemical analysis, infrared spectroscopy, low temperature nitrogen adsorption-desorption technique and solid diffuse reflection absorption spectroscopy were used to characterize the prepared host-guest composite material (MCM-41)-RhB. The composite material shows luminescence and has the potentiality as luminescent material.

*Corresponding author. E-mail: Zhaiqingzhou@163.com, zhaiqingzhou@hotmail.com

EXPERIMENTAL

Reagent

The reagents and materials used were as follows: tetraethylorthosilicate (TEOS, Fluka, Switzerland); cetyltrimethylammonium bromide (CTMAB, Changzhou Xinhua Research Institute for Reagent, China); rhodamine B (RhB, Shanghai Third Chemical Plant, China, 1.0×10^{-4} M), sodium hydroxide (Kaiyuan Kangyuan Chemical Plant, China, 2.0 M) and deionized water. All chemicals were of analytical reagents unless stated otherwise.

Sample preparation. The host nanometer MCM-41 molecular sieve was synthesized by hydrothermal method using tetraethylorthosilicate as silica source and CTMAB as structure-directing agent. A 1.0 g of CTMAB was added into 480 mL of deionized water at 80 °C under vigorous stirring. When the solution became homogeneous, 3.5 mL of sodium hydroxide solution was added with stirring. After the solution became homogeneous, 5 mL of TEOS was slowly added dropwise, giving rise to a white slurry. Then the reaction mixture was kept at 80 °C for 2 h with stirring. The resulting solid was recovered by filtration, extensively washed with deionized water, and dried at ambient temperature. The template was removed by calcination at 500 °C for 4 h [8]. The uncalcined and calcined samples were designed as S-no and S, respectively. The calcined MCM-41 sample was used as a host to incorporate the guest by liquid-phase grafting method. 0.400 g of the calcined nanometer molecular sieve MCM-41 was added into 40 mL of 1.0×10^{-4} M rhodamine B solution at ambient temperature with stirring for 72 h. Then the resulting product was extensively washed with deionized water, until free RhB disappeared. Finally, the prepared materials were dried at 40 °C for 6 h. The prepared host-guest composite material was (nanometer MCM-41)-rhodamine B, which was designed as S-RhB. A distribution of main size of the S-RhB sample ranged from 120 to 180 nm by scanning electric microscopy (JEOL JSM-5600L SEM) and the primary particles of the sample presented ball crystals (images not shown).

Characterization techniques. The powder X-ray diffraction patterns were recorded using a Siemens D5005 (Germany) X-ray diffractometer, where Cu target K_{α} -ray ($\lambda = 0.15418$ nm) and operating at 30 kV and 20 mA) was used as X-ray source. Data were collected between the 2θ range of $0.4^{\circ} - 10^{\circ}$ with a resolution of 0.02° . Infrared spectra were recorded on a 5DX-FTIR spectrometer (Nicolet, USA) with potassium bromide pellets (99 wt. % of KBr). Low temperature nitrogen adsorption and desorption isotherms were obtained at 77 K on a Micromeritics ASAP 2010M system (Mike Company, USA). The data were calculated in terms of the model of Broekhoff and de Boer (BdB) [16]. Surface area and pore volume were calculated by BET (Brunauer-Emmett-Teller) [17] and BJH (Barett-Joyner-Halenda) [18] procedures, respectively. The UV-Vis diffuse reflection absorption spectra were measured using a Perkin-Elmer Lambda spectrometer (Mike Company, USA). Fluorescence excitation and emission spectra were recorded on a SPEX FL-2T2 spectrofluorometer (SPEX Company, USA).

RESULTS AND DISCUSSION

Powder X-ray Diffraction. Figure 1 shows the powder X-ray diffraction patterns of samples. The XRD patterns for all three samples display four obvious diffraction peaks (100), (110), (200) and (200), which are characteristic of MCM-41 and in good agreement with those in the literature [8]. The size of the prepared MCM-41 molecular sieves determined by TEM was 120-180 nm (Images not shown). The diffraction peaks intensities of the calcined molecular sieve increase, showing that the ordered degree of the lattice arrangement of the molecular sieve further increases. In Figure 1, one major peak together with three additional small peaks can be observed and attributed to the (110), (200) and (210) of the MCM-41. In the calcined molecular

sieve sample, the intact framework was retained. However, their diffraction peak intensities enhance. This shows that the ordered degree increases for the calcined MCM-41. Figure 1-c shows the X-ray diffraction pattern of the (nanometer MCM-41)-RhB sample. The diffraction peaks of the nanometer MCM-41 and (nanometer MCM-41)-RhB samples are at 2.64° and 2.15° , respectively. Compared with the host nanometer MCM-41, the diffraction peaks of the (nanometer MCM-41)-RhB sample shift slightly to lower angles. The results show that the framework of the molecular sieve was kept intact and ordered in the host-guest (nanometer MCM-41)-(rhodamine B) composite material. However, the diffraction intensity of the prepared composite sample decreases, suggesting that the ordered degree of the sample decreases compared with that of the nanometer MCM-41 host.

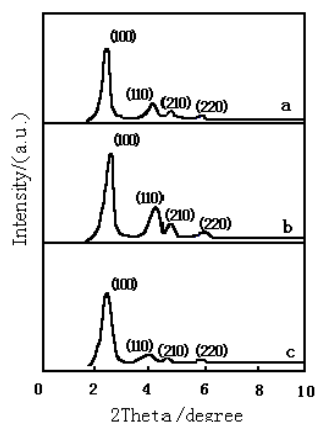


Figure 1. X-ray diffraction patterns of the samples. (a) nanometer MCM-41 uncalcined (S-no); (b) nanometer MCM-41 calcined (S); (c) S-RhB.

Chemical analysis. The content of the MCM-41 molecular sieve in the prepared host-guest composite material was determined by molybdosilicate blue photometry [19]. The content of the RhB was obtained by the difference subtraction. The prepared sample contains 3.1 % (mass fraction) of RhB.

IR spectra. Figure 2 shows the infrared spectra of the samples. In Figure 2-a, for the calcined nanometer MCM-41 sample the peak at 1080 cm^{-1} can be attributed to the asymmetrical stretching vibration of Si-O-Si bond of the MCM-41. The symmetrical stretching vibration located at 803 cm^{-1} . The bending vibration of Si-O-Si bond lies at 446 cm^{-1} . The peak at 970 cm^{-1} can be attributed to the symmetrical stretching vibration of terminal group Si-OH [20]. In Figure 2-b, for the (nanometer MCM-41)-RhB sample the corresponding peaks are at 1091, 798, 466, 961 cm^{-1} . Thus, the framework of the MCM-41 in the host-guest composite material (nanometer MCM-41)-RhB was kept intact. Some infrared peaks of the host-guest composite material at 1091, 466 cm^{-1} shifted toward longer wavenumber relative to those of the host at 1080, 446 cm^{-1} . The incorporation of rhodamine B changed the surface state of the molecular sieve. The RhB further increased the dispersion extent of the surface component of the molecular sieve. This made the surface adsorption center increased and caused absorption peak intensity to increase. The increase in the dispersion made decrease in the density of the electric cloud of the bond Si-O-Si and caused these characteristic peaks to move to higher wavenumber. Compared with the peaks at 970, 803 cm^{-1} of the host material, some infrared peaks of the host-guest composite material move to smaller wavenumber 961, 798 cm^{-1} , respectively. The

movement of the absorption wavenumber to smaller one resulted from the fact that the electrons of the -CH bond of the RhB transfer to the bond Si-OH of the molecular sieve. This made the bond order of Si-OH decrease. However, the characteristic infrared peaks of the host nanometer MCM-41 are retained in the prepared host-guest composite material. This indicates that the framework of the MCM-41 is still retained in the host-guest composite material.

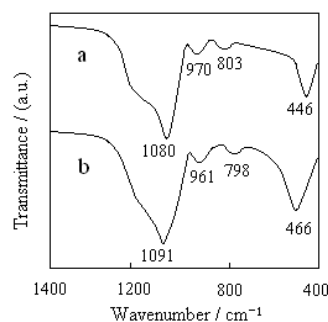


Figure 2. Infrared spectra of the samples. (a) S (nanometer MCM-41 calcined); (b) S-RhB.

Nitrogen adsorption-desorption isotherms. Figure 3 shows the low temperature nitrogen adsorption-desorption isotherms and pore size distribution patterns of the nanometer MCM-41 and (nanometer MCM-41)-RhB samples. The isotherms of the two samples can be classified as a type of Langmuir isotherm according to the IUPAC (International Union of Pure and Applied Chemistry) nomenclature [21], which are a typical adsorption of mesoporous material with a complete filling of the mesoporous system at very low partial pressure. At lower relative pressure ($P/P_0 = 0.25/0.30$), the quantities of the adsorption for the MCM-41 and the (nanometer MCM-41)-RhB increase and the obvious steep increases. This increase shows the uniformity of the mesoporous size distribution. Slope of the adsorption curve of the (nanometer MCM-41)-RhB sample is less than that of the nanometer MCM-41 over $P/P_0 = 0.25/0.30$. However, it is still big. This results from the good distribution of the rhodamine B in the channel of the host. When the relative pressure is over the range of $P/P_0 = 0.30/0.90$, the adsorptions of nitrogen in the nanometer MCM-41 (Figure 3-A-a) and the (nanometer MCM-41)-RhB samples (Figure 3-A-b) reach equilibrium, which show longer adsorption terraces. Another obvious steep increases in Figure 3-A-a and Figure 3-A-b are at a relative pressure $P/P_0 = 0.90/1.0$, which results from the capillary condensation caused by the pores among the particles.

Figure 3-B shows the pore size distribution of the samples, suggesting that the prepared sample (nanometer MCM-41)-RhB has the ordered structure of one-dimensional pore channel. The curve was close to Gaussian distribution. The decrease in the BET surface area and pore volume of the molecular sieve host in the (nanometer MCM-41)-RhB sample suggests that some of the pore space of the MCM-41 be occupied by the inclusion of rhodamine B. Thus, this shows that the rhodamine B has been properly confined inside the channels of the nanometer MCM-41 host. The structure information about the samples derived from nitrogen adsorption-desorption data are listed in Table 1.

Table 1. Pore structure parameters of the samples.

Sample	d_{100}^a (nm)	a_0^b (nm)	BET surface area ($m^2 \cdot g^{-1}$)	Pore volume ^c ($cm^3 \cdot g^{-1}$)	Pore size ^d (nm)
S (Nanometer MCM-41 calcined)	3.34	3.85	961	0.566	2.29
S-RhB	3.56	4.11	903	0.510	2.19

^aCrystal face spacing. ^bUnit cell parameter, $a_0 = 2/(3)^{1/2}d_{100}$. ^cBJH adsorption cumulative volume of pores. ^dPore size calculated from the adsorption branch.

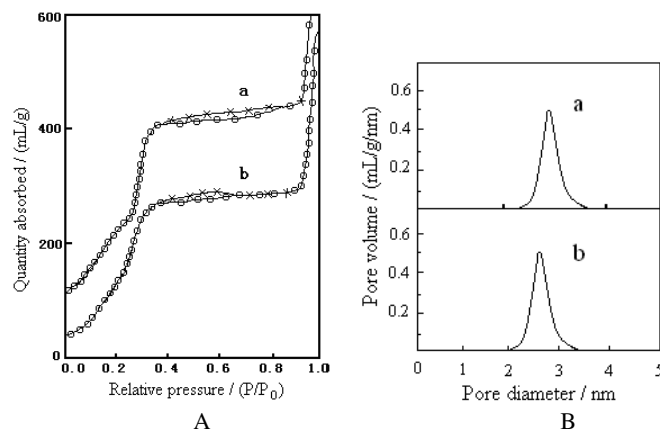


Figure 3. Low temperature nitrogen adsorption–desorption isotherms and pore size distribution patterns of the samples (○ adsorption; × desorption). (a) S (nanometer MCM-41 calcined); (b) S-RhB.

UV-VIS spectroscopy. The UV-Vis diffuse reflection absorption spectra of the samples are shown in Figure 4. There is no absorption from the nanometer MCM-41 host. From the figure it can be seen that the absorption peaks of the (nanometer MCM-41)-RhB and RhB samples locate at 567 nm and 611 nm, respectively. The absorption of the S-RhB sample does not come from the molecular sieve host. This absorption contributes from the nanometer RhB confined in the channels of the MCM-41 molecular sieve. The absorption peak of the (nanometer MCM-41)-RhB sample has a blue shift of 44 nm relative to that of the RhB bulk. The blue-shift can be attributed to a stereoconfinement effect of channels of the MCM-41 molecular sieve. This also suggests that the RhB guest be successfully incorporated into the channels of the nanometer MCM-41 molecular sieve host in the prepared host-guest composite material.

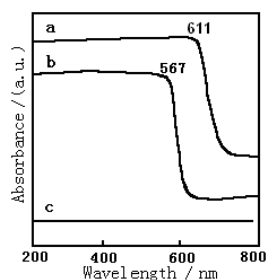


Figure 4. Diffuse reflectance absorption spectra of the samples. (a) RhB; (b) nanometer MCM-41 calcined (S)-RhB; (c) S.

Luminescence. The molecular sieve host does not show any luminescence. However, the prepared host-guest composite material (nanometer MCM-41)-RhB exhibits luminescence (Figure 5). The excitation peak of the (nanometer MCM-41)-RhB sample is at 270 nm, and the emission peak of the (nanometer MCM-41)-RhB sample locates at 582 nm. The luminescent intensity of the material is weak, showing that the non-radiative process is very strong in the host-guest material and the population inversion is very easily established. The strong interaction of electron-photon in the sample results in the Stokes displacement and makes the

spectrum bands broaden. The prepared host-guest nanocomposite material (nanometer MCM-41)-RhB has the potentiality as luminescence material.

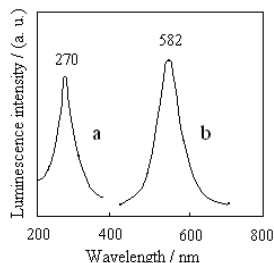


Figure 5. Luminescence of the (nanometer MCM-41)-RhB sample. (a) excitation spectrum ($\lambda_{em} = 582$ nm); (b) emission spectrum ($\lambda_{ex} = 270$ nm).

CONCLUSIONS

The host-guest nanocomposite material (nanometer MCM-41)-rhodamine B was successfully prepared by liquid grafting method. A series of characterizations including powder X-ray diffraction, chemical analysis, infrared spectroscopy, low temperature nitrogen adsorption-desorption technique, and solid diffuse reflection absorption spectroscopy showed that the framework in the prepared host-guest composite material was still retained and kept highly ordered. The guest rhodamine B locates inside the channels of the MCM-41 in the host-guest material. The prepared host-guest nanocomposite material (nanometer MCM-41)-rhodamine B has the potentiality as luminescence material.

REFERENCES

1. Feynman, R.P. *Science* **1991**, 254, 1300.
2. Stankic, S.; Sterrer, M.; Hoffmann, P. *Nano. Lett.* **2005**, 5, 1889.
3. Mardilovich, P.; Kornilovitch, P. *Nano. Lett.* **2005**, 5, 1899.
4. Barbic, M. *Nano. Lett.* **2006**, 5, 787.
5. Zhai, Q.Z. *Nanotechnology*, Weapon Industry Press: Beijing; **2006**; p 386.
6. Kresge, C.T.; Leonowicz, M.E.; Roth, W.J.; Vartuli, J.C.; Beck, J.S. *Nature* **1992**, 359, 710.
7. Beck, J.S.; Vartuli, J.C.; Roth, W.J., Leonowicz, E.; Kresge, C.T.; Schumitt, K.D.; Chu, T.W. *J. Am. Chem. Soc.* **1992**, 114, 10834.
8. Cai, Q.; Luo, Z.S.; Pang, W.Q. *Chem. Mater.* **2001**, 13, 258.
9. Stucky, G.D.; Mac Dougall, J.E. *Science* **1990**, 247, 669.
10. Ozin, G.A.; Kuperman, A.; Stein, A. *Angew. Chem.* **1992**, 4, 511.
11. Zhai, Q.Z. *Acta Phys.-Chim. Sinica* **1998**, 14, 1116.
12. Benedikt, L.; Marco, L.; Adeline, R. *J. Mater. Chem.* **2002**, 12, 528.
13. Brien, S.O.; Tudor, J.; Low, S.B. *Chem. Commun.* **1997**, 641.
14. Isabel, D.; Belen, G.; Beatriz, A. *Chem. Mater.* **2003**, 15, 1073.
15. Cai, J.Y.; Zhai, Q.Z., Yu, H. *Bull. Chin. Ceram. Soc.* **2006**, 25, 30.
16. Broekhoff, J.C.P.; Deboer, J.H. *J. Catal.* **1968**, 10, 307.
17. Brumauer, S.; Emmett, P.H.; Teller, E. *J. Am. Chem. Soc.* **1938**, 60, 309.
18. Barrett, E.P.; Joyner, L.G.; Halenda, P.P. *J. Am. Chem. Soc.* **1951**, 73, 373.
19. Zhai, Q.Z.; Kim, Y.C. *Chin. J. Spectrosc. Lab.* **1998**, 15, 82.
20. Xu, R.R.; Pang, W.Q.; Tu, K.G. *Zeolite Molecular Sieves Structure and Synthesis*, Jilin University Press: Changchun; **1987**; p 94.
21. IUPAC *Pure. Appl. Chem.* **1957**, 87, 603.